

## Analysis of the Transformations Temperatures of Helicoidal Ti-Ni Actuators Using Computational Numerical Methods

Carlos Augusto do N. Oliveira<sup>a\*</sup>, Alvaro Antonio Ochoa Villa<sup>a</sup>, Cezar Henrique Gonzalez<sup>a</sup>,  
Pablo Batista Guimarães<sup>b</sup>, Rodrigo José Ferreira<sup>b</sup>, Severino Leopoldino Urtiga Filho<sup>a</sup>,  
Niedson José da Silva<sup>b</sup>, José Orlando Silveira Rocha<sup>a</sup>

<sup>a</sup>Department of Mechanical Engineering, Centre for Technology and Geosciences,  
Federal University of Pernambuco – UFPE, Av. Acadêmico Hélio Ramos, s/n,  
Cidade Universitária, CEP 50740-530, Recife, PE, Brazil

<sup>b</sup>Department of Mechanics, Federal Institute of Pernambuco – IFPE, Av. Luiz Freire 500,  
Cidade Universitária, CEP 50740-540, Recife, PE, Brazil

Received: January 19, 2012; Revised: January 29, 2013

The development of shape memory actuators has enabled noteworthy applications in the mechanical engineering, robotics, aerospace, and oil industries and in medicine. These applications have been targeted on miniaturization and taking full advantage of spaces. This article analyses a Ti-Ni shape memory actuator used as part of a flow control system. A Ti-Ni spring actuator is subjected to thermomechanical training and parameters such as transformation temperature, thermal hysteresis and shape memory effect performance were investigated. These parameters were important for understanding the behavior of the actuator related to martensitic phase transformation during the heating and cooling cycles which it undergoes when in service. The multiple regression methodology was used as a computational tool for analysing data in order to simulate and predict the results for stress and cycles where the experimental data was not developed. The results obtained using the training cycles enable actuators to be characterized and the numerical simulation to be validated.

**Keywords:** *shape memory effect, Ti-Ni actuators, multiple regression analysis*

### 1. Introduction

The development of smart actuators using a shape memory effect has become very common in industrial applications<sup>1,2</sup>. The main reason for this is that these make it possible to generate very compact actuator systems. Ti-Ni alloys are an important class of alloys, due to their shape memory phenomena (one-way shape memory effect, two-way shape memory effect, and their superelasticity)<sup>3,4</sup>. This class of material has been used as a raw material for actuator devices in mechanical engineering and many other areas, including medicine, robotics, aerospace, oil and natural gas industries.

Phase transformation fatigue and mechanical cycling fatigue are important phenomena associated to smart spring actuators. Understanding shape memory degradation involving fatigue for different levels of stress and a given number of cycles is valuable information in application such as to have when studying flow control valves. The main objective of this research is to predict phase transformation parameters by using computational numerical methods monitoring the behavior of parameters for different levels of stress and number of cycles. The numerical methods proposed in this research have already been used to describe

others phenomena such as drying phenomena. Research using function fit was developed depending on different conditions such as temperature, drying speed and relative humidity presented good coherence with experimental values<sup>5</sup>. Statistical parameters such as the Correlation Coefficient, Mean Bias Error and Root Mean Square Error, were used to determine the drying rate of figs<sup>6</sup>. Another paper that tackled the same subject was written by Menges and Ertekin (2006)<sup>7</sup>. In another engineering area, Hellmann et al. (1998) put forward a method to prevent the behavior of chillers by using a simple algebraic function<sup>8</sup>. The main research result was to improve the curve fit for absorption systems<sup>9</sup>.

The results obtained address the influence of the training process on the behavior of the actuator, where modifications were observed in the critical transformation temperatures and a variation in yield from shape memory due to reconfiguration of the internal defects<sup>10-12</sup>. Data analysis using numerical methods emerged as an efficient method for projecting the behavior parameters of the actuator with non-experimentally assessed tensions. The numerical method applied made the results obtained interesting and coherent as to improving understanding of the functionality of the actuators.

\*e-mail: cano.oliveira@gmail.com

## 2. Experimental Procedure

### 2.1. Experimental part

This research investigated the performance of the shape memory effect on commercial Ti-50.4at% Ni, 0.89 mm in diameter wire. This material was homogenized at 500 °C for a period of 24 hours and then cooled in water at 25 °C.

Differential scanning calorimetry (DSC) technique was used to identify the direct and reverse martensitic transformation temperatures ( $M_s$  and  $M_f$ , the starting and finishing temperatures of direct martensitic transformation on cooling from austenite to martensite,  $A_s$  and  $A_f$ , the beginning and the end temperatures of reverse martensitic transformation on heating) in the range of temperatures between -60 °C and 100 °C, at a rate of 10 °C/min<sup>-1</sup>. This method was used to analyze the material in the as-received and heat treated conditions.

The wire was used to produce actuator with a helical spring by shaping the wire around a screw, and then submitting the set to heat treatment at 500 °C for 24 hours<sup>13,14</sup>. The actuator obtained had a 6.0 mm outer diameter, 4 active coils and was approximately 6.0 mm long.

Figure 1 shows the schematic configuration of the system used to conduct the thermomechanical training of the actuator. The device consists of an element to fix the spring, a pulley, a non-extensible wire, a rod to transmit the applied load, the load, the Linear Variation Displacement Transducer (LVDT) sensors, the temperature sensors and a data acquisition set Monitored by a computer. The load is applied at 20 °C elongating the spring (as shown latter in the results topic, at 20 °C, the wire is in the martensitic state) and then heated to 90 °C (above  $A_f$ , also shown later) contracting the spring. If this cooling and heating cycle is repeated several times, it is called training process. The heating and cooling rate was estimated to be around 5 °C/min and 3 °C/min, respectively.

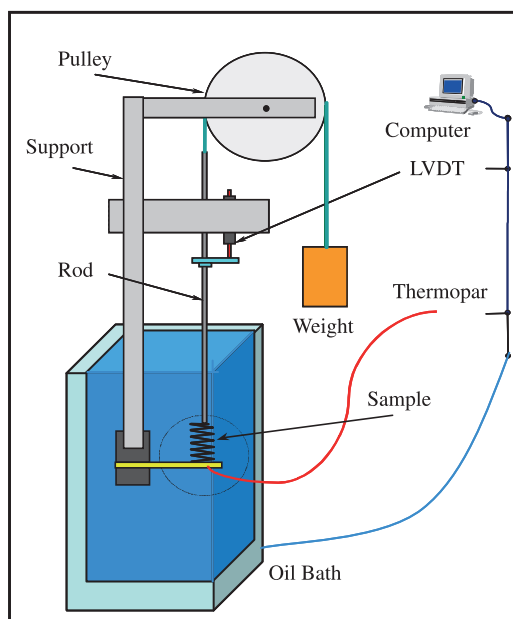
The evaluation of the mechanical behavior and the shape memory effect of the actuator was performed by repeating 40 times the heating and cooling cycle for each applied load (stress) of 35, 70, 105, 135, 170 and 200 MPa<sup>15,16</sup>.

Figure 2 shows the main parameters from a generic thermo-elastic deformation curve. The tangent rule identifies the critical transformation temperatures ( $A_s$ ,  $A_f$ ,  $M_s$  and  $M_f$ ), thermo-elastic deformations in millimeters ( $\epsilon_t$ ) and the linear dislocation between cycles (X)<sup>15</sup>.

### 2.2. Numerical part

In this section the study seeks to verify the consistency of the results regarding the behavior of the actuator for non-experimentally analyzed stresses due to the limitation of the device as to producing fast heating and cooling of the cycles.

The modeling procedure consists of a multiple regression applied to the experimental data obtained in order to predict numerical values that were not evaluated during the experimental training procedure. The setting used was a non-linear method based on Levenberg-Marquardt and Gauss-Newton. Matlab software was used as a development tool by creating subroutines to calculate the general settings<sup>17</sup>.



**Figure 1.** Diagram of the system used to conduct on the training process of the actuator.

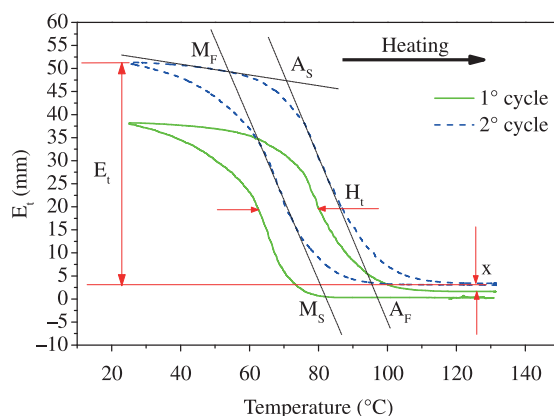


**Figure 2.** Tangent rule for thermo-elastic deformation as function of temperature curves<sup>15</sup>.

Initially, non-linear regressions were performed to calculate the coefficients for known stress. Thereafter, the results were evaluated by linear regression for the total adjustment, i.e., the verification of the simulated and experimental data, for each value of stress and applied number of cycles.

To determine the coefficients of the equations for each critical transformation temperature ( $A_s$ ,  $A_f$ ,  $M_s$ ,  $M_f$ ), a non-linear regression was performed for each of the forty cycles. Then calculation of the general coefficients as a function of the each applied stress was made in order to obtain a general numerical model that would predict the temperatures evolution as function of number of cycles, i.e.,  $A_s$ ,  $A_f$ ,  $M_s$  and  $M_f$ .

Equations 1 to 4 were defined to simulate the behavior of the critical temperatures of the transformation as function

of the cycles evaluated. The general coefficients are shown in Equations 5 to 8. The adjustment consists of coefficients that vary with the stress and the number of cycles.

$$A_s = a \cdot \text{cycle}^3 + b \cdot \text{cycle}^2 + c \cdot \text{cycle} + d \quad (1)$$

$$M_s = a \cdot \text{cycle}^3 + b \cdot \text{cycle}^2 + c \cdot \text{cycle} + d \quad (2)$$

$$A_f = a \cdot \text{cycle}^3 + b \cdot \text{cycle}^2 + c \cdot \text{cycle} + d \quad (3)$$

$$M_f = a \cdot \text{cycle}^3 + b \cdot \text{cycle}^2 + c \cdot \text{cycle} + d \quad (4)$$

where a, b, c and d, were the temperature coefficients of the equations, which were implicit functions of the tension applied to the material by means of training. A linear form was used due to the simplicity of the analysis<sup>5-7,18</sup>.

$$a = a_0 + a_1 \cdot \text{tension} \quad (5)$$

$$b = b_0 + b_1 \cdot \text{tension} \quad (6)$$

$$c = c_0 + c_1 \cdot \text{tension} \quad (7)$$

$$d = d_0 + d_1 \cdot \text{tension} \quad (8)$$

In order to validate the equations and the data obtained by multiple regressions method, the following statistical parameters were used:

- Correlation coefficient ( $r^2$ ): defines the accuracy of the simulated values in relation to the experimental ones as a function of the straight line, i.e., the proximity of all values being the same for each stress condition during the evolution of the cycles<sup>19</sup>;
- Mean bias error (MBE): a total residue, between the experimental and simulated values<sup>19</sup>;
- Root mean square error (RMSE), the total squared residue between the experimental and simulated data<sup>19</sup>.

Equations 9, 10 and 11 were used to calculate the statistical parameters mentioned above.

$$r^2 = \frac{\text{Values}_{\text{experimental}} - \text{Values}_{\text{simulated}}}{\text{Values}_{\text{experimental}}} \quad (9)$$

$$\text{MBE} = \frac{1}{N} * \sum_{i=1}^N (\text{Values}_{\text{experimental}} - \text{Values}_{\text{simulated}}) \quad (10)$$

$$\text{RMSE} = \left[ \frac{1}{N} * \sum_{i=1}^N (\text{Values}_{\text{experimental}} - \text{Values}_{\text{simulated}})^2 \right]^{(1/2)} \quad (11)$$

Where:

$\text{Values}_{\text{experimental}}$ ; Values from experimental data.

$\text{Values}_{\text{simulated}}$ ; Values from simulated data.

N; number of experimental data.

## 3. Results and Discussions

### 3.1. Calorimetric analysis

Figure 3 shows curves representing heat flow as a function of temperature for the as-received condition. As

far as no transformation peaks were observed, it is supposed that the wire is in as drawn condition, that is, work hardened condition inhibiting the reversibility of direct and reverse martensitic transformation<sup>4,20</sup>.

Figure 4 shows the calorimetric curves that designate phase transformation after heat treatment at 500 °C for 24 hours. On heating, a reverse martensitic transformation peak is observed with  $A_s$  and  $A_f$  temperatures of 56 and 73 °C, respectively. On cooling, a direct martensitic transformation temperature with  $M_s$  and  $M_f$  of 39 and 26 °C are observed. The respective transformations enthalpies on heating and on cooling were  $\Delta H_H = 25.0$  J/g and  $\Delta H_C = 26.0$  J/g, a typical values for NiTi shape memory alloys.

### 3.2. Training process of the actuators

Thermomechanical cycles were performed in a silicone oil thermal bath as shown elsewhere<sup>15</sup>. A constant shear stress was applied to the actuator wire and this enabled the recovery of the shape of the activator to be assessed as a function of the applied stress and the number of cycles. The training process was developed in this research to induce martensite variants reconfiguration in accordance to the axis along the stress is applied<sup>11,21-24</sup>.

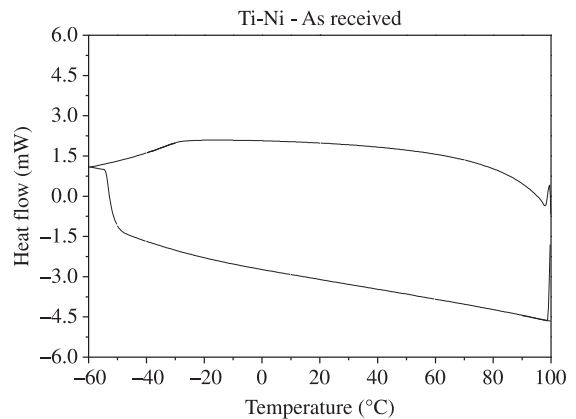


Figure 3. DSC curves of the as received material.

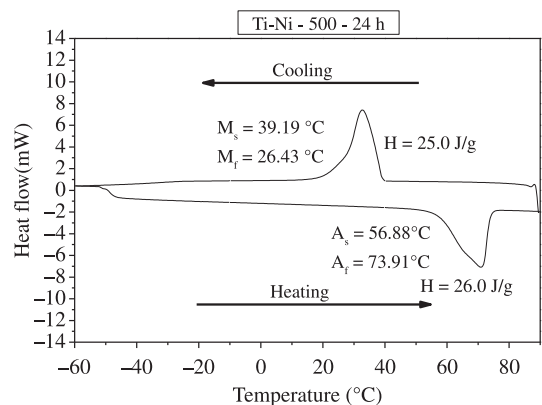


Figure 4. Calorimetric curve for the sample when heat treated at 500 °C for 24 hours.

The heating and cooling cycles brought about by training enable the critical temperature, thermal hysteresis and the thermo-elastic strain to be studied. The thermo-elastic strain is able to indicate the efficiency of the shape memory effect by means of linear displacement.

Figure 5 shows the strain curves as a function of temperature for nominal shear stress of 35, 70, 105, 135, 170 and 200 MPa.

The analysis of the strain curves identifies that 35 MPa stress exhibited approximately 13.0 mm of thermo-elastic deformation after 40 training cycles and that stresses of 70 and 105 MPa showed a continuous trend for thermo-elastic deformation to increase. The 70 MPa applied stress exhibited a thermo-elastic increase from 26.0 to 28.0 mm

and 105 MPa stress showed an increase from 35.0 to 41.0 mm. Thermo-elastic deformation behavior showed an increase for 35, 70 and 105 MPa stress. Above these parameters the tendency starts to decrease and thermal hysteresis starts to increase. Narrow thermo-elastic results were observed for 35 and 70 MPa. The main reason for this behavior was the small stress applied that was insufficient to totally induce martensitic variants orientation.

Figure 6 shows the thermo-elastic behavior as a function of the number of cycles for the actuators and Figure 7 shows the  $M_s$  and  $A_s$  temperatures as that for applied stress.

The start temperature of the martensitic transformation ( $M_s$ ) tends to increase with stress in accordance with the Clausius-Clapeyron relation<sup>4,22,23</sup>. During the training

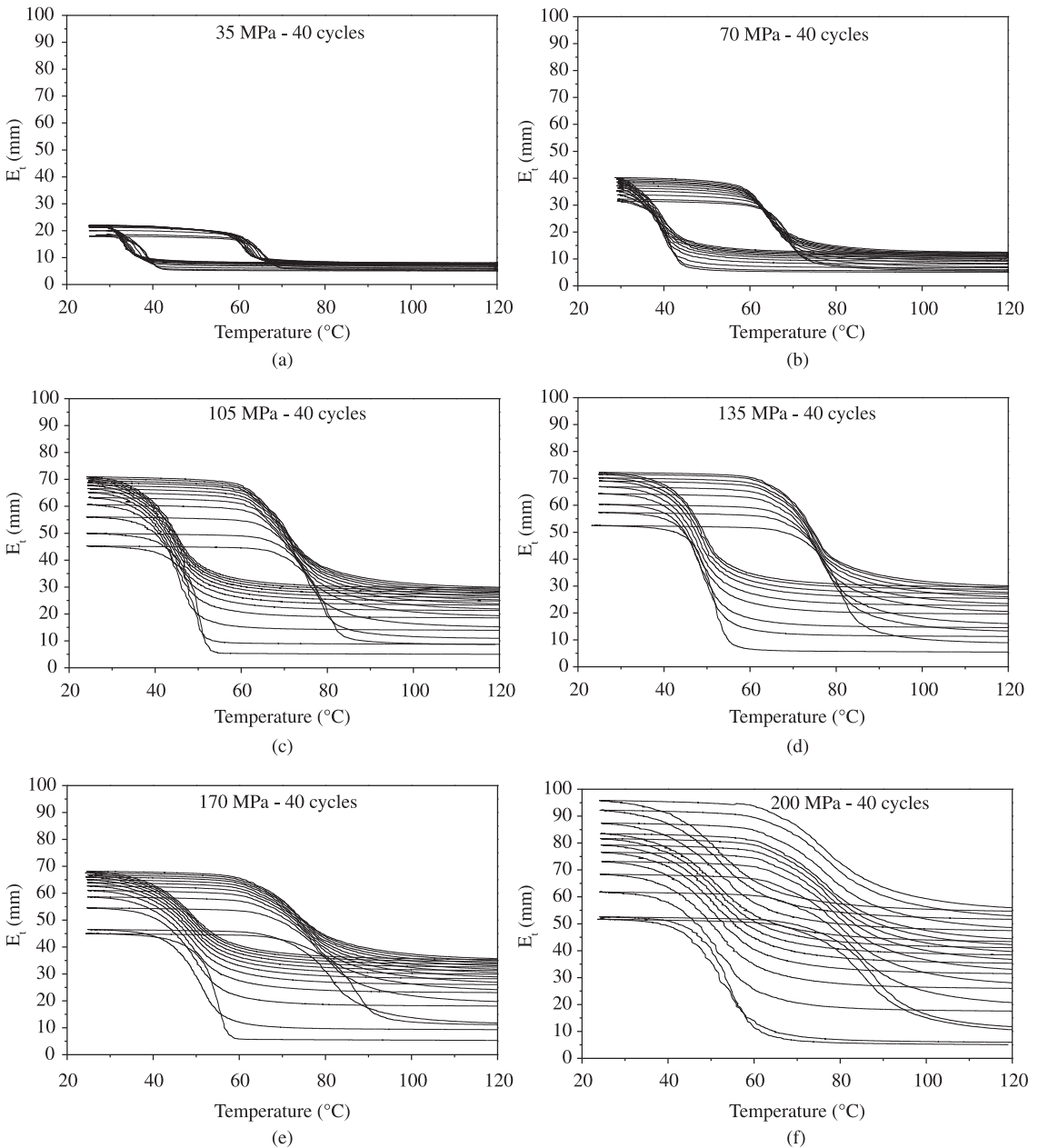


Figure 5. Strain as a function of temperature for. a) 35 MPa, b) 70 MPa, c) 105 MPa, d) 135 MPa, e) 170 MPa and f) 200 MPa.

process,  $M_s$  temperature decreases with number of cycles for small stress value, while for stress above 135 MPa the evolution is the inverse. In the first case, the  $M_s$  temperature decreases because of dislocation reorientation which modifies the internal stress and points the martensitic variant in the preferential direction<sup>16,24</sup>. In the second case, the  $M_s$  temperature increases for high stress due to fast martensitic reconfiguration and exhaustion (practically all martensitic variants were immediately activated by stress)<sup>23</sup>. The results for  $A_s$  temperature showed that this parameter decreases for all stresses studied. However, for a small stress the variation shown is almost 5 °C and for higher stresses, the variation is 12 °C.

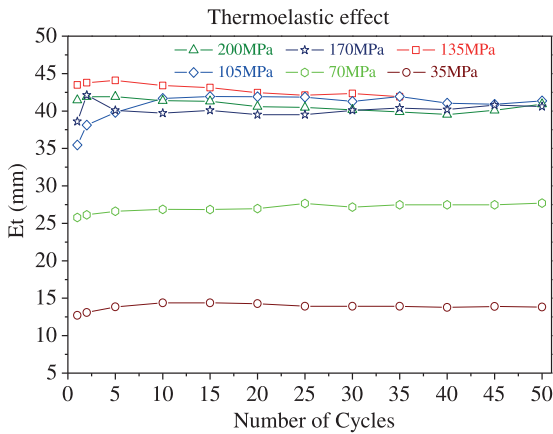
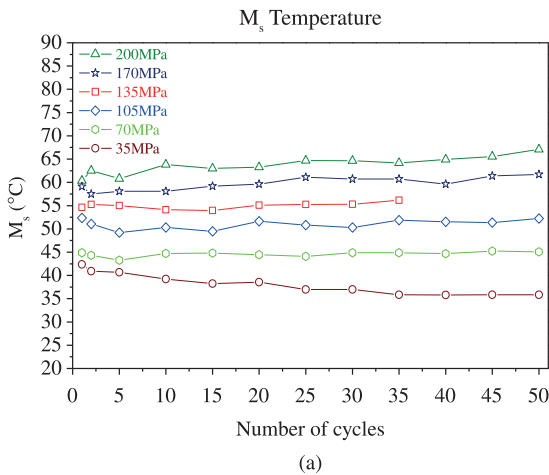


Figure 6. Thermo-elastic deformation behavior as function of number of cycles for 35, 70, 105, 135, 170 and 200 MPa stress.



The increase behavior observed on the  $M_s$  temperature and the decrease behavior on the  $A_s$  temperature results in the hysteresis reduction. This phenomenon is a result of an efficient martensitic orientation process due to the thermomechanical training process that induces more martensitic variants activation which needs less energy to initiate transformation<sup>10,11</sup>.

3.3. Modeling the temperature curves ( $A_s, A_f, M_s, M_f$ )

The development of the curve fit in Matlab enabled the linear correlation of the statistical parameters to be obtained. The Mean Bias Error and Root Mean Square Error were obtained to validate the regressions applied to the critical temperatures of the phase transformation. Table 1 presents these parameters as a function of each of the critical transformation temperatures studied for the actuators developed.

As can be seen in Table 1, for all temperature data, the values of the statistical parameters enabled it to be verified that the regressions applied provided satisfactory results. The values shown in Table 1 certify the validity of this model for the non-linear regression, since it has a large  $r^2$  value, almost unity, and small values for both the mean bias error and the root mean square error.

3.3.1. Temperature ( $A_s$ )

Figure 8 shows the temperature curves adjusted by the regressions of the experimental values with the simulated ones for each applied stress and the results of the linear regressions as a function of the number of cycles. The experimental values are represented by solid lines and the

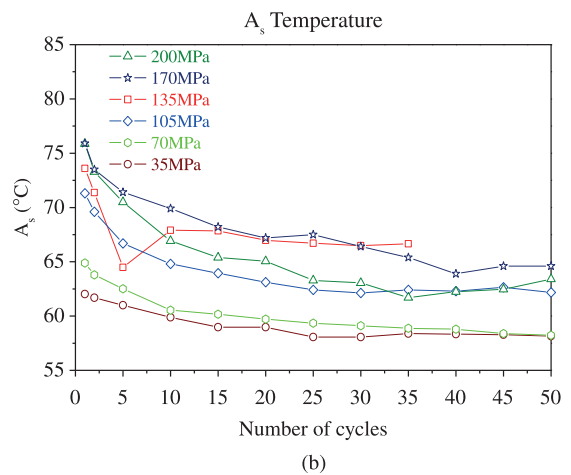


Figure 7. Temperature behavior as function of number of cycles to 35, 70, 105, 135, 170 and 200 MPa stress. a)  $M_s$  and b)  $A_s$ .

Table 1. Results of the statistical parameters used for validating the multiple regression applied to the adjustment of the temperature curves.

Temperature	$r^2$	MBE	RMSE
$A_s$	0,95778652	$7,74339101 \times 10^{-08}$	0,23754001
$A_f$	0,99546039	$2,10233868 \times 10^{-09}$	0,16440879
$M_s$	0,98994356	$-2,61632067 \times 10^{-08}$	0,14160765
$M_f$	0,94080045	$1,85334061 \times 10^{-07}$	0,18382697

simulated ones by symbols. In this case, the adjustments were made individually. It was observed that the behavior of the curves was similar, since the simulated values are close to the experimental ones, with a maximum relative error of 4% at 200 MPa stress. This error is due to the behavior of the equations for this load which led to the final correlations obtaining this value, but even that it is considered a very good fit.

On comparing the simulated values with the general equation for temperature  $A_s$  (Equation 1), and the experimental values for this temperature (Figure 8) it is observed that the multiple regression methodology applied reveals that the simulated values met a 95% probability within the range limited between maximum and minimum values, thus ensuring an optimal setting according to the function of a straight line ( $x = y$ )<sup>6</sup>.

Figure 9 shows the data for the residual  $A_s$  temperature as a function of the simulated values based on the multiple regression of the experimental data and the comparison of these curves after the multiple regression of the data for temperature  $A_s$ .

The data presented in Figure 9 a enable the observation to be made that the residue confirms a good fit was

made - the residues from a fitted curve are defined as the differences between the experimental data and the simulated data at each load value - since this behavior does not show a systematic pattern, thus showing the efficiency of the model applied. On comparing the simulated values with the general equation for  $A_s$  temperature (Equation 1), and the experimental values for this temperature (Figure 9b) it is observed that the multiple regression methodology applied reveals that the simulated values met a 95% probability within the range limited between maximum and minimum values, thus ensuring an optimal setting according to the function of a straight line ( $x = y$ )<sup>6</sup>. The comparison of the residues with the simulated values provides a maximum relative error of 3% and a minimum one of 0.2%, which once again validates the model used to simulate the parameter of  $A_s$  temperature for the tension range between 35 and 200 MPa.

3.3.2. Temperature ( $M_s$ )

Figure 10 shows the curves of the temperature  $M_s$  adjusted by the regressions of the experimental values with the simulated ones for each stress applied and the results of the linear regressions as function of the number of cycles.

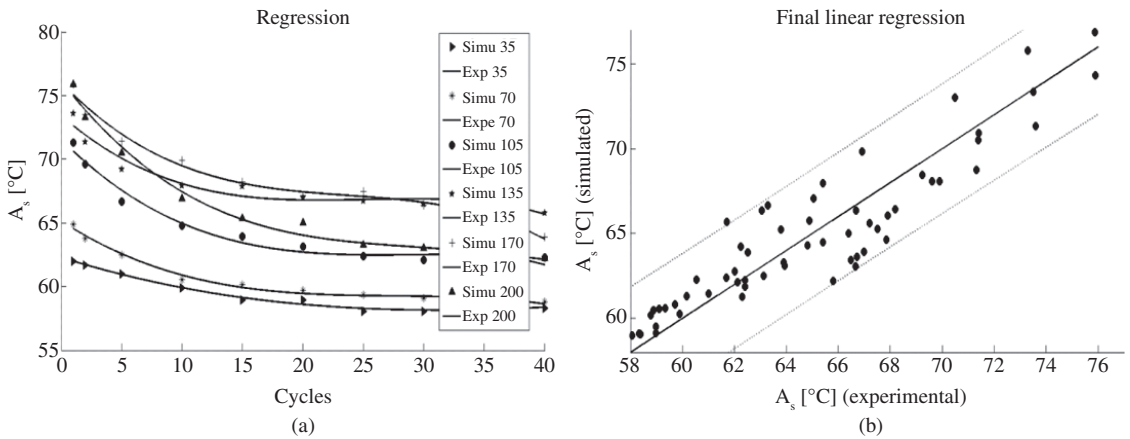


Figure 8. (a) Comparison of the experimental values with those adjusted by regression for temperature  $A_s$  and (b) Linear regression of the experimental and simulated values of the temperature  $A_s$  for different applied tensions.

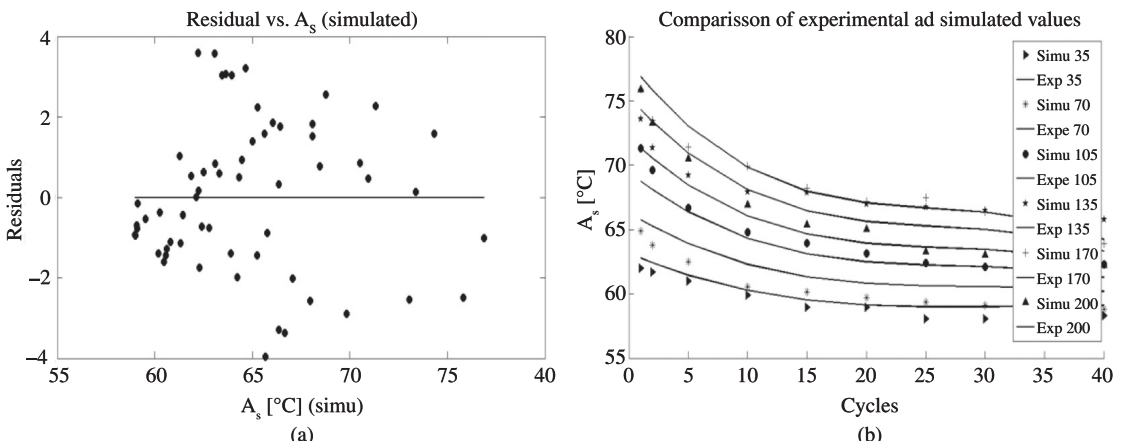


Figure 9. (a) Comparison of the residual values versus the simulated values of temperature  $A_s$  by means of the multiple regression and (b) final comparison of the experimental and simulated values of temperature  $A_s$  as function of the evolution of cycles and tensions.

The experimental values are represented by solid lines and the simulated ones by symbols. In this case, the adjustment is made individually, and it is observed that the behavior of the curves is generally similar, since the simulated values are close to the experimental ones, with a maximum relative error of 3% for 105 MPa stress. This error is due to the behavior of the equations for this load which led to the final correlations obtaining this value, but even that it is considered a very good fit.

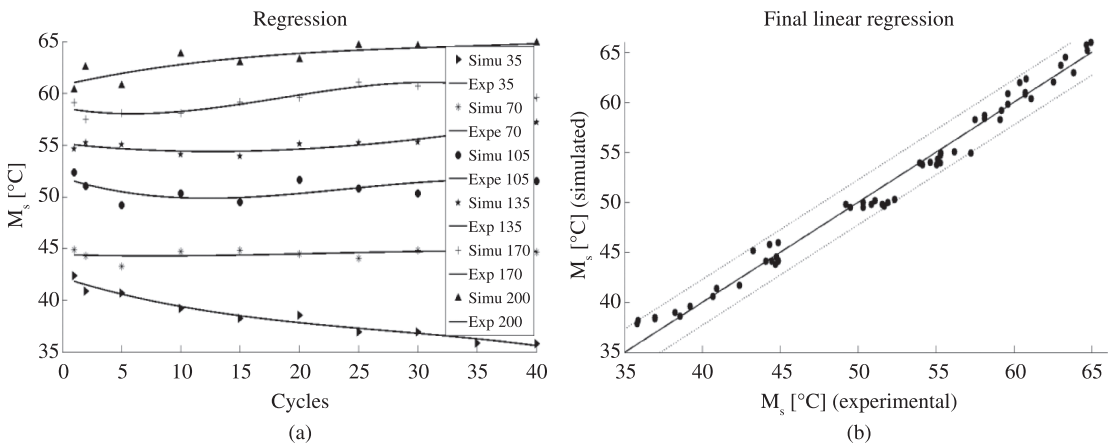
On comparing the simulated values with the general equation of temperature  $M_s$  (Equation 2), and the experimental values of the temperature  $A_s$ , (Figure 10), it is observed that the multiple regression methodology applied reveals that the simulated values met a 95% probability within the range limited between maximum and minimum values, thus ensuring an optimal setting according to the function of a straight line ( $x = y$ )<sup>6</sup>.

Figure 11 shows the data of the residual temperature  $M_s$  as a function of the simulated values based on the multiple regression of the experimental data and the comparison of these curves after the multiple regression of the data for temperature  $M_s$ .

The data presented in Figure 11.a enable it to be observed that the residue confirms the good fit achieved, since this behavior does not show a systematic pattern, thus showing the efficiency of the applied model. The comparison of the simulated residues with the simulated values provides a maximum relative error of 6% and a minimum one of 0.6 %, which once again validates the model used for simulating of the temperature parameter  $A_s$  for the tension range between 35 and 200 MPa.

### 3.3.3. Temperatures ( $A_f$ and $M_f$ )

The data on fitting the curves to the temperature parameters of  $A_f$  and  $M_f$  showed a similar behavior to that obtained for the parameters  $A_s$  and  $M_s$ . However, by analyzing the comparison of the residues results, relative errors of 2% maximum and 0.13% minimum were obtained for the parameter  $A_f$ .  $M_f$  had maximum and minimum errors of 7% and 0.7% respectively. These errors are due to the behavior of the equations for these loads that led to the final correlations obtained for these values, but even that it is considered a very good fit.



**Figure 10.** (a) Comparison of the experimental values with the adjusted ones by regression for temperature  $M_s$  and (b) Linear regression of the experimental and simulated values of temperature  $M_s$  for different applied tensions.

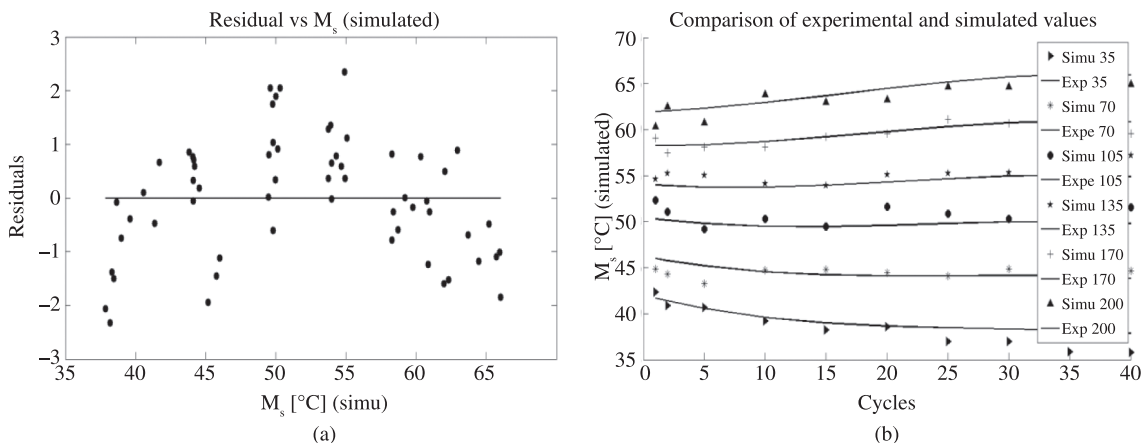


**Figure 11.** (a) Comparison of the residue versus the simulated values of temperature  $M_s$  by the multiple regression and (b) final comparison of the experimental and simulated values of temperature  $M_s$  as a function of the evolution of the cycles and tensions.

Figure 12 shows the result of the final comparison between the experimental and simulated values of the temperature parameters  $A_f$  and  $M_f$ .

3.4. Simulation

Figures 13 and 14 show the behavior of temperatures ( $A_s, M_s, A_f, M_f$ ) for stress ranging from 35 MPa to 200 MPa

and the evolution of the cycles, as per the equations provided by the multiple regression of the experimental values.

Using the results of the computational simulation, Figures 13 and 14 show that the behavior of all temperatures ( $A_s, M_s, A_f, M_f$ ) follows a set pattern, thus obeying the reaction of the material to external stimuli that impose real changes on transformation temperatures. Therefore,

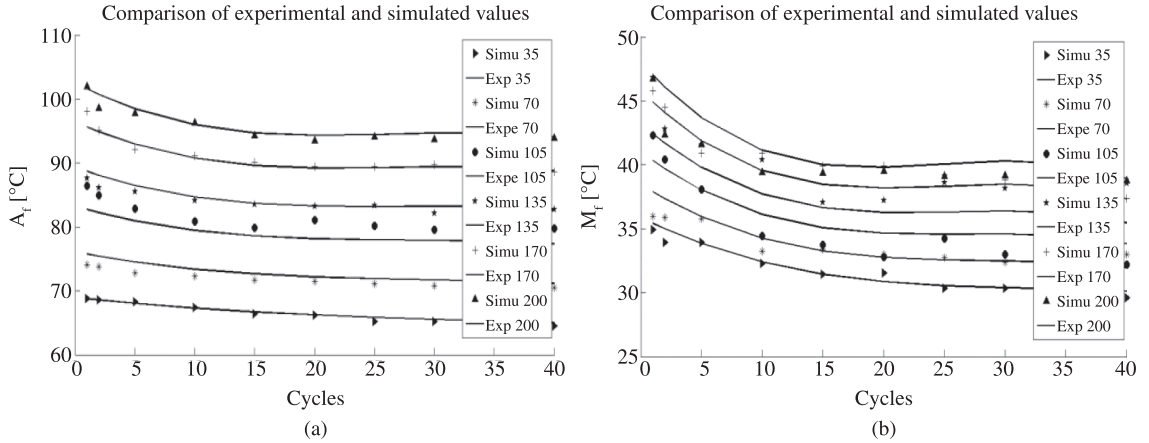


Figure 12. Final comparison of experimental and simulated values of the parameters of temperature. (a)  $A_f$  and (b)  $M_f$ .

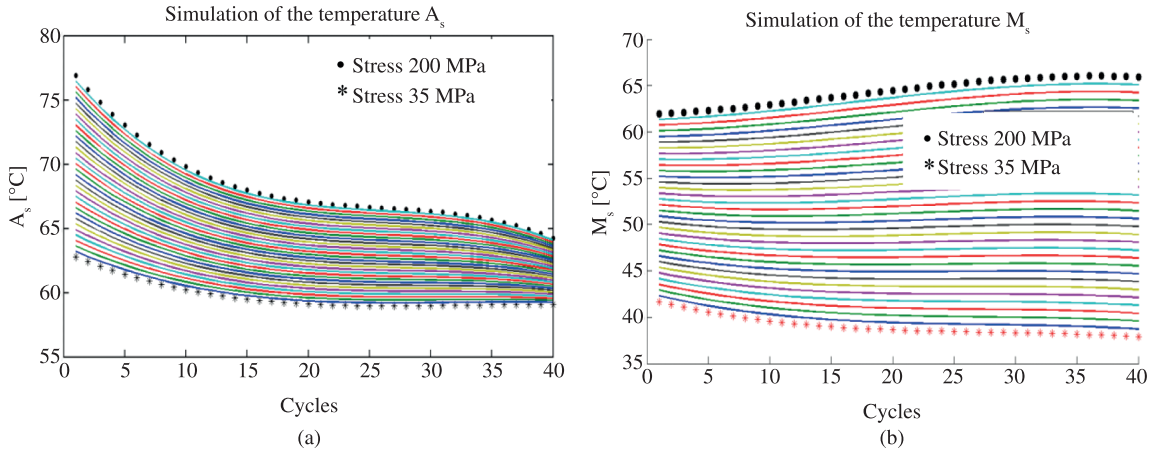


Figure 13. Behavior of the temperature parameters for stress between 35 MPa and 200 MPa. (a)  $A_s$  and (b)  $M_s$ .

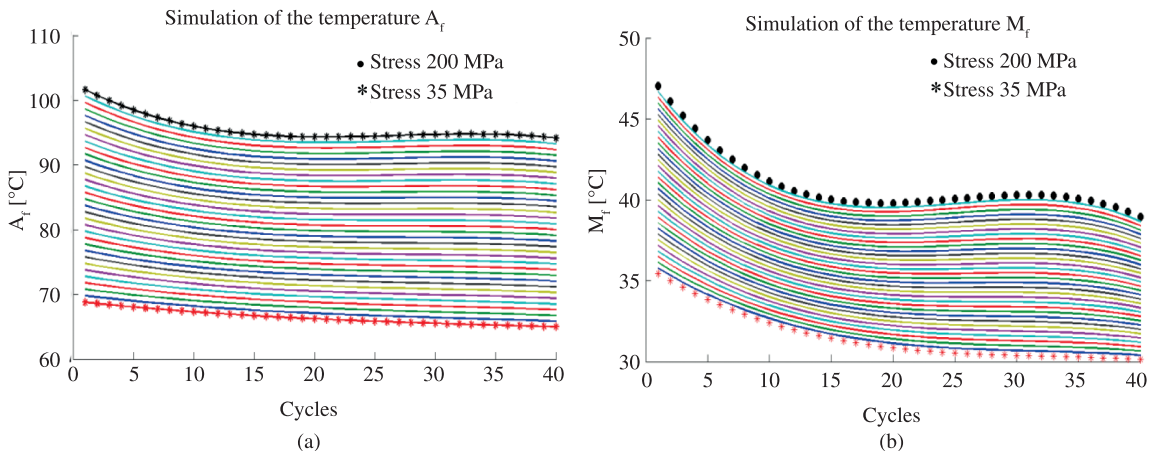


Figure 14. Behavior of the temperature parameters for stress between 35 MPa and 200 MPa. (a)  $A_f$  and (b)  $M_f$ .

we have as the default (standard) behavior, reducing the  $A_s$  temperatures with the evolution of the cycles and their increasing when using stress of a higher intensity. Thus, the  $M_s$  temperatures remain showing a mild trend of increasing with the evolution of the cycles and when tensions of higher intensity are used. This behavior is also seen at  $A_f$  and  $M_f$  temperatures. Therefore, multiple regression using temperature data, cycles and tensions of thermomechanical training in a Ti-Ni actuator was able to produce results by generating information suitable for simulation testing that would take too long to be studied by means of conventional experimental analysis.

#### 4. Conclusions

Based on the results, we conclude that:

- This paper showed the experimental results for the training process. Transformation temperatures and thermal hysteresis were modified due to the applied stress and the evolution of the cycles. Stress fields and martensitic reconfiguration induced changes in temperature transformation due to the applied stress and number of cycle's evolution. These phenomena were observed because of the variation in temperature

and thermo-elastic deformation during the training procedure;

- The curve fitting methodology applied is valid to simulate the conditions, where the experimental data was not developed on a conventional way, of training in a Ti-Ni actuator by thermomechanical analysis, thus facilitating the characterization of phase transformation of the actuator according to the condition that was imposed; and
- The numerical results showed that the behavior of all temperatures ( $A_s$ ,  $M_s$ ,  $A_f$  and  $M_f$ ) follows a definite pattern and obey the material reaction to external stimuli that impose modifications on the transformation temperature.

#### Acknowledgements

The authors are grateful to the Brazilian agencies: Coordenação de Aperfeiçoamento de Pessoal de Nível Superior (CAPES), Conselho Nacional de Desenvolvimento Científico e Tecnológico (CNPq) and Fundação de Amparo à Ciência e Tecnologia do Estado de Pernambuco (FACEPE) for their financial support and the scholarships they awarded to this research project.

#### References

1. Andersen D, Pedersen A and Sangesland SAS. *Detailed study of shape memory alloys in oil well applications*. Trondheim: SINTEF Petroleum Research; 1999.
2. Gore J, Bowles A, Maylin M, Chandrasekaran L, Forsyth D and Buyers M. High temperature shape memory alloy actuators through mechanical treatments for an oil & gas down-hole valve. *Industrial and Commercial Applications of Smart Structures Technologies, SPIE Digital Library*, 2008. v. 6930. <http://dx.doi.org/10.1117/12.776306>
3. Delaey L, Krishnan RV, Tas H and Warlimont H. Thermoelasticity, pseudoelasticity and the memory effects associated with martensitic transformations. *Journal of Materials Science*. 1974; 9:14. <http://dx.doi.org/10.1007/BF00552939>
4. Otsuka K and Ren X. Physical metallurgy of Ti-Ni-based shape memory alloys. *Progress in Materials Science*. 2005; 50(5):511-678. <http://dx.doi.org/10.1016/j.pmatsci.2004.10.001>
5. Akpınar EK and Bicer Y. Mathematical modelling of thin layer drying process of long green pepper in solar dryer and under open Sun. *Energy Conversion and Management*. 2008; 49(6):1367-1375. <http://dx.doi.org/10.1016/j.enconman.2008.01.004>
6. Xanthopoulos G, Oikonomou, N and Lambrinos G. Applicability of a single-layer drying model to predict the drying rate of whole figs. *Journal of Food Engineering*. 2007. 81(3):553-559. <http://dx.doi.org/10.1016/j.jfoodeng.2006.11.033>
7. Menges HO and Ertekin C. Mathematical modeling of thin layer drying of Golden apples. *Journal of Food Engineering*. 2006; 77(1):119-125. <http://dx.doi.org/10.1016/j.jfoodeng.2005.06.049>
8. Hellmann HM, Schweigler C and Ziegler F. The characteristic equations of absorption chillers. In: *Proceedings of the International Sorption Heat Pump Conference*; 1999; Munich. Munich; 1999. p. 4.
9. Gutiérrez-Urueta G, Rodríguez P, Ziegler F, Lecuona A and Rodríguez-Hidalgo MC. Extension of the characteristic equation to absorption chillers with adiabatic absorbers. *International Journal of Refrigeration*. 2012; 35(3):709-718. <http://dx.doi.org/10.1016/j.ijrefrig.2011.10.010>
10. Gonzalez CH, Oliveira CAN, Pina EAC, Urtiga Filho SL, Araújo Filho OO and Araújo CJ. Heat Treatments and Thermomechanical Cycling Influences on the R-Phase in Ti-Ni Shape Memory Alloys. *Materials Research-Ibero-American Journal of Materials*. 2010; 13(3):325-331. <http://dx.doi.org/10.1590/S1516-14392010000300008>
11. Paula ASC, Canejo JPH, Martins RMS and Braz Fernandes FM. Effect of thermal cyclin on the transformation temperature ranges of a Ni-Ti shape memory alloy. *Materials Science and Engineering: A*. 2004; 378(1-2):92-96. <http://dx.doi.org/10.1016/j.msea.2003.11.057>
12. Somsen C, Zähres H, Kastner J, Kakeshita T and Saburi T. Influence of thermal annealing on the martensitic transitions in Ni-Ti shape memory alloys. *Materials Science and Engineering: A*. 1999; 273:310-314. [http://dx.doi.org/10.1016/S0921-5093\(99\)00362-7](http://dx.doi.org/10.1016/S0921-5093(99)00362-7)
13. De Araújo CJ, Silva E and Gonzalez CH. Thermal alarm using a shape memory alloy helical spring. In: *Proceedings of the 16th Brazilian Congress of Mechanical Engineering Uberlândia*; 2005; Uberlândia. Uberlândia; 2005. v. 15, p. 8.
14. Oliveira CAN, Gonzalez CH, De Araújo CJ, Pina EAC, Urtiga Filho SL and Araújo Filho OO. Caracterização do Efeito Memória de forma Reversível de Molas de Cu-Zn-Al. *Revista Eletrônica de Materiais e Processos*. 2009; 4(3):76-86.
15. Oliveira CAN, Gonzalez CH, Araújo CJ, Araújo Filho OO and Urtiga Filho SL. Thermoelastic Properties on Cu-Zn-Al Shape Memory Springs. *Materials Research*. 2011; 13(2):219-223. <http://dx.doi.org/10.1590/S1516-14392010000200016>
16. De Araújo CJ, Gonzalez CH, Morin M and Guénin G. Influence of the Mechanical Loading History on the Stress Assisted Two Way Memory Effect in a Ti-Ni-Cu Alloy. In: *Anais do 61º*

- Congresso Anual da Associação Brasileira de Metalurgia e Materiais*; 2006; Rio de Janeiro. Rio de Janeiro; 2006. p. 8.
17. Steven C and Raymond C. *Numerical Methods for Engineers*. McGraw-Hill College; 2009.
  18. Togrul IT and Pehlivan D. Mathematical modelling of solar drying of apricots in thin layers. *Journal of Food Engineering*. 2002; 55(3):209-216. [http://dx.doi.org/10.1016/S0260-8774\(02\)00065-1](http://dx.doi.org/10.1016/S0260-8774(02)00065-1)
  19. Chaudhuri S and Drton M. *On the Bias and Mean-square error of the Sample Minimum and the Maximum Likelihood Estimator for Two Ordered Normal Means*. Washington: Department of Statistics, University of Washington; 2003.
  20. Oliveira CAN, Gonzalez CH, Pina EAC, Urtiga Filho SL, Araújo Filho OO and De Araújo CJ. Precipitates formation in Ti-Ni equiatomic alloys due to annealing heat treatment. *Materials Science Forum*. 2010; 643:49-54. <http://dx.doi.org/10.4028/www.scientific.net/MSF.643.49>
  21. Wang ZG, Zu XT, Dai JY, Fu P and Feng XD. Effect of Thermomechanical Training Temperature on the Two-Way Shape Memory Effect of Ti-Ni and Ti-Ni-Cu Shape Memory Alloys Springs. *Materials Letters*. 2003; 57(9-10):1501-1507. [http://dx.doi.org/10.1016/S0167-577X\(02\)01014-5](http://dx.doi.org/10.1016/S0167-577X(02)01014-5)
  22. Huang W and Goh HB. On the long-term stability of two-way shape memory alloy trained by reheat treatment. *Journal of Materials Science Letters*. 2001; 20(19):1795-1797. <http://dx.doi.org/10.1023/A:1012543402147>
  23. Lahoz R, Gracia-Villa L and Puertolas JA. Training of the two-way shape memory effect by bending in NiTi alloys. *Journal of Engineering Materials and Technology-Transactions of the Asme*. 2002; 124(4):397-401. <http://dx.doi.org/10.1115/1.1495001>
  24. Villafana A, Masse M, Portier R and Pons J. Thermomechanical testing machine conceived for the study of shape memory alloys. Application to the training and testing of the two-way memory effect. *Journal de Physique IV France*. 1997; 7(C5):655-660. <http://dx.doi.org/10.1051/jp4:19975104>